Article No. jmbi.1999.3430 available online at http://www.idealibrary.com on IDEAL® J. Mol. Biol. (2000) 295, 1265–1273

JMB

Orienting Domains in Proteins Using Dipolar Couplings Measured by Liquid-state NMR: Differences in Solution and Crystal Forms of Maltodextrin Binding Protein Loaded with β-Cyclodextrin

Nikolai R. Skrynnikov*, Natalie K. Goto, Daiwen Yang, Wing-Yiu Choy Joel R. Tolman, Geoffrey A. Mueller and Lewis E. Kay*

Contribution from the Protein Engineering Network Centres of Excellence and Departments of Medical Genetics Biochemistry and Chemistry University of Toronto, Toronto, Ontario, Canada, M5S 1A8

**Corresponding authors*

Protein function is often regulated by conformational changes that occur in response to ligand binding or covalent modification such as phosphorylation. In many multidomain proteins these conformational changes involve reorientation of domains within the protein. Although X-ray crystallography can be used to determine the relative orientation of domains, the crystal-state conformation can reflect the effect of crystal packing forces and therefore may differ from the physiologically relevant form existing in solution. Here we demonstrate that the solution-state conformation of a multidomain protein can be obtained from its X-ray structure using an extensive set of dipolar couplings measured by triple-resonance multidimensional NMR spectroscopy in weakly aligning solvent. The solution-state conformation of the 370-residue maltodextrin-binding protein (MBP) loaded with β-cyclodextrin has been determined on the basis of one-bond ^{15}N-H^N, ^{15}N-$^{13}C'$, $^{13}C^{\alpha}$-$^{13}C'$, two-bond $^{13}C'$-H^N, and three-bond $^{13}C^{\alpha}$-H^N dipolar couplings measured for 280, 262, 276, 262, and 276 residues, respectively. This conformation was generated by applying hinge rotations to various X-ray structures of MBP seeking to minimize the difference between the experimentally measured and calculated dipolar couplings. Consistent structures have been derived in this manner starting from four different crystal forms of MBP. The analysis has revealed substantial differences between the resulting solution-state conformation and its crystal-state counterpart (Protein Data Bank accession code 1DMB) with the solution structure characterized by an 11(±1)° domain closure. We have demonstrated that the precision achieved in these analyses is most likely limited by small uncertainties in the intradomain structure of the protein (ca 5° uncertainty in orientation of internuclear vectors within domains). In addition, potential effects of interdomain motion have been considered using a number of different models and it was found that the structures derived on the basis of dipolar couplings accurately represent the effective average conformation of the protein.

Keywords: protein structure and dynamics; domain orientation; triple-resonance multidimensional NMR; dipolar couplings; maltodextrin-binding protein

Introduction

In many multidomain proteins, the relative orientation of domains can change in response to ligand binding or covalent modification such as phosphorylation. These conformational changes often control biological processes such as enzymatic catalysis or signal transduction (Pawson,

Abbreviations used: MBP, maltodextrin-binding protein; NOE, nuclear Overhauser effect; DC, dipolar coupling; TROSY, transverse relaxation-optimized spectroscopy.

E-mail addresses of the corresponding authors: kay@bloch.med.utoronto.ca; nikolai@pound.med.utoronto.ca

0022-2836/00/51265–9 $35.00/0

1995). One goal of structural studies is, therefore, to describe the average orientations of domains and how they change in response to various factors (Gerstein *et al*., 1994). X-ray crystallography can provide an accurate description of molecular structure as it exists in the crystal lattice, but the orientation of domains in this case can be influenced by crystal packing forces. As a result, the position of domains as established by X-ray crystallography may differ from the average position that is observed in solution (Shilton *et al*., 1996).

Until recently, NMR studies of proteins in solution have been limited to relatively small single-domain molecules comprised of approximately 250 residues or less. However, the development of multidimensional ^{15}N, ^{13}C, ^{2}H triple-resonance experiments (Bax, 1994; Gardner & Kay, 1998), and the establishment of methods for the measurement of residual dipolar couplings (Tolman *et al*., 1995; Tjandra *et al*., 1996a; Wang *et al*., 1998; Yang *et al*., 1999) have facilitated the study of multidomain proteins, in particular, making it possible to determine average domain orientations in solution (Losonczi *et al*., 1999; Fischer *et al*., 1999; Markus *et al*., 1999).

The 370-residue maltodextrin binding protein (MBP) from *Escherichia coli* which has been investigated in this work consists of two domains which are comparable in size and connected by two β-strands and a relatively long stretch of α-helix. X-ray studies have demonstrated that the relative orientation of the two domains depends on the type of ligand bound (Spurlino *et al*., 1991; Sharff *et al*., 1992, 1993; Quiocho *et al*., 1997). The existence of open and closed conformations is crucial for MBP's role in the signal transduction cascade that regulates both maltodextrin uptake and chemotaxis (Mowbray & Sandgren, 1998).

X-ray data show that conformational changes in MBP and other members of the periplasmic binding protein family can be described as hinge rotations, i.e. rigid-body rotations of one domain with respect to the other that do not alter intradomain structure (Sharff *et al*., 1992; Van Aalten *et al*., 1997). Extensive NMR studies have established that the intradomain structure of maltose-binding protein (MBP) in solution is essentially the same as that found in the crystal form (Zwahlen *et al*., 1998; Gardner *et al*., 1998; Yang & Kay, 1999). Hence, hinge rotations can also be used to describe conformational differences between solution and crystal forms of MBP.

Despite the fact that several weak interdomain NOEs can be detected in the proximity of the hinge region of MBP, the relative position of the two domains cannot be accurately determined from these data. This problem is addressed here by using the orientational information contained in an extensive set of one-bond ^{15}N-H^N, ^{15}N-$^{13}C'$, $^{13}C^{\alpha}$-$^{13}C'$, two-bond $^{13}C'$-H^N and three-bond $^{13}C^{\alpha}$-H^N dipolar couplings which were measured in a sample of MBP with β-cyclodextrin dissolved in dilute liquid-crystalline solvent (Yang *et al*., 1999). Dipolar coupling data were used to adjust the relative orientation of domains in X-ray crystal structures of MBP, thus obtaining the solution-state conformation of the protein. Notably, it was found that the conformation of β-cyclodextrin-bound MBP in solution differs from the crystal form, with the solution structure related to the X-ray structure *via* an 11° domain closure.

Dipolar couplings

The dipolar coupling (DC) between two spin-1/2 nuclei, I and M, arising from the partial alignment of a protein molecule in anisotropic solvent, can be expressed as (Bastiaan *et al*., 1987; Tjandra & Bax, 1997; Clore *et al*., 1998):

$$D_{IM} = D_0^{IM} A_a S\{(3\cos^2\theta - 1) + (3/2)R\sin^2\theta\cos 2\phi\} \quad (1)$$

where $D_0^{IM} = -(1/2\pi)(\mu_0/4\pi)\hbar\gamma_I\gamma_M\langle r_{IM}^{-3}\rangle$ is the dipolar interaction constant, S is the order parameter that reflects isotropic averaging due to fast local dynamics, A_a is the axial component of the molecular alignment tensor, R is its rhombicity parameter, and θ and φ are polar angles that specify the orientation of the IM internuclear vector with respect to the molecular alignment frame. The orientation of the alignment frame is defined relative to a fixed molecular frame, such as the X-ray coordinate frame, and is expressed by the Euler angles {α, β, γ}.

Equation (1) shows that DCs characterize vector orientation in a position-independent manner and hence can be considered as global structural parameters. For example, two parallel N-H^N vectors give rise to equal D_{NH} values regardless of their location in the polypeptide chain. This property distinguishes DCs from local parameters such as NOEs and J-couplings, which involve spins that are close together in space, making DCs especially useful for the determination of global protein folds in solution. Here we discuss the use of DCs to refine the conformation of the multidomain protein MBP.

Orienting domains in MBP

In this approach, we generated solution-state conformations of MBP by applying hinge rotations to X-ray crystal structures of the protein. A minimization algorithm was designed to search for the hinge rotation that provides the best agreement between the measured and calculated DC values (see Materials and Methods for details). Four different sets of X-ray coordinates were used in these analyses representing two open structures (the Protein Data Bank accession numbers 1OMP (Sharff *et al*., 1992) and 1DMB (Sharff *et al*., 1993)) and two closed structures (1ANF (Quiocho *et al*., 1997) and 4MBP (Quiocho *et al*., 1997)). Prior to the analysis, all structures were transferred into the same coordinate frame by superimposing their

C-domains and hinge rotations were subsequently applied to N-domains.

The results obtained from the conformational search using the dipolar couplings measured for MBP in solution with β-cyclodextrin are summarized in Table 1A and shown schematically in Figure 1(a). The hinge rotations are represented in the Figure as sequences of three orthogonal rotations, so that the relative position of two spheres in Figure 1(a) gives the amplitude of closure, twist, and bending that transforms one structure into another (see Materials and Methods for definitions). The cluster of spheres in the center of the plot represents the liquid-state conformation of MBP as derived from the four different X-ray structures. The results in Figure 1(a) show good convergence, permitting calculation of an average solution structure. The average solution structure of β-cyclodextrin-loaded MBP is related to its crystal counterpart 1DMB *via* 11(±1)° closure, 1(±3)° twist, and 1(±2)° bending. The error estimates in the above results are obtained from the comparison of four solution-state conformations derived from the different X-ray crystal structures listed above.

It should be noted that the conformation obtained on the basis of DCs is not unique, since DC values remain invariant when a domain is rotated by 180° about the x, y, or z axis of the alignment frame (this reflects four equivalent choices for a right-handed alignment frame: {α, β, γ}, {α, β, 180° + γ}, {180° + α, 180° − β, 180° − γ}, and {180° + α, 180° − β, 360° − γ}) (Brüschweiler *et al.*, 1995). However, only one of the four resulting structures is represented by a hinge rotation with a moderate amplitude ω, whereas the three others correspond to large-amplitude rotations (ω ca 180°). For proteins such as MBP it is improbable that the solution conformation differs so significantly from the crystal form; in general, the latter three solutions can usually be discarded.

The residual deviations between the measured and calculated DC values, χ^2, are encoded by color in Figure 1(a) and listed in Table 1A. As expected, solution structures obtained from the minimization procedure match the experimental data better than the original X-ray structures, with the lowest χ^2 values found for the solution structures derived from 1OMP and 1ANF. These two structures are shown in Figure 2, together with the parent X-ray structures. Although the search algorithm started with two visibly different X-ray conformations (Figure 2(a) and (b)), very similar solution confor-

Table 1. Transformation parameters describing the relationship between solution-state conformations generated on the basis of DC data and X-ray crystal forms of MBP

		Starting crystal structure	(Θ, Φ)[a]; ω[b] Relative to starting structure	Closure; twist; bending[c] Relative to 1OMP	Relative to 1DMB	χ^2 (10^3 Hz^2)[d]
A	Static solution-state conformation Figure 1(a)	1OMP	(109°, 108°); 13°	13°, 0°, −4°	10°, 0°, −3°	2.27 [4.12]
		1DMB	(127°, 105°); 13°	15°, 4°, −4°	12°, 4°, −4°	4.00 [5.75]
		1ANF	(101°, 119°); −22°	15°, 0°, 0°	12°, −1°, 0°	2.34 [6.41]
		4MBP	(90°, 113°); −24°	13°, 4°, 0°	10°, 4°, 1°	2.99 [6.77]
B	Dynamic solution-state conformation Figure 1(b)	1OMP	(79°, 105°); 17°	14°, −8°, −5°	11°, −9°, −5°	2.28 [4.12]
		1DMB	(83°, 102°); 17°	17°, −7°, −6°	14°, −7°, −6°	4.08 [5.75]
		1ANF	(104°, 121°); −21°	15°, −2°, −1°	12°, −2°, 0°	2.40 [6.41]
		4MBP	(78°, 111°); −24°	13°, 5°, 1°	10°, 4°, 1°	3.03 [6.77]

[a] Prior to the analysis, all X-ray structures were transferred into the coordinate frame of 1OMP as described in Materials and Methods. The orientations of the hinge axes, (Θ, Φ), are therefore reported in this common coordinate frame, rather than in the original coordinates from the protein database. This allows for direct comparison of (Θ, Φ) angles obtained with different starting structures.

[b] A positive amplitude of hinge rotation ω corresponds to a clock-wise rotation.

[c] The orientations of closure, twist, and bending axes in the coordinate system of 1OMP are described by the following pairs of polar angles: (109°, 124°), (159°, 279°), and (82°, 212°). See Materials and Methods for derivation of the axes.

[d] χ^2 is a measure of agreement between the experimental DC values and DC values calculated using the optimized solution-state conformation, see the text. Shown in square brackets are the minimum χ^2 values obtained using the original (unaltered) X-ray structures.

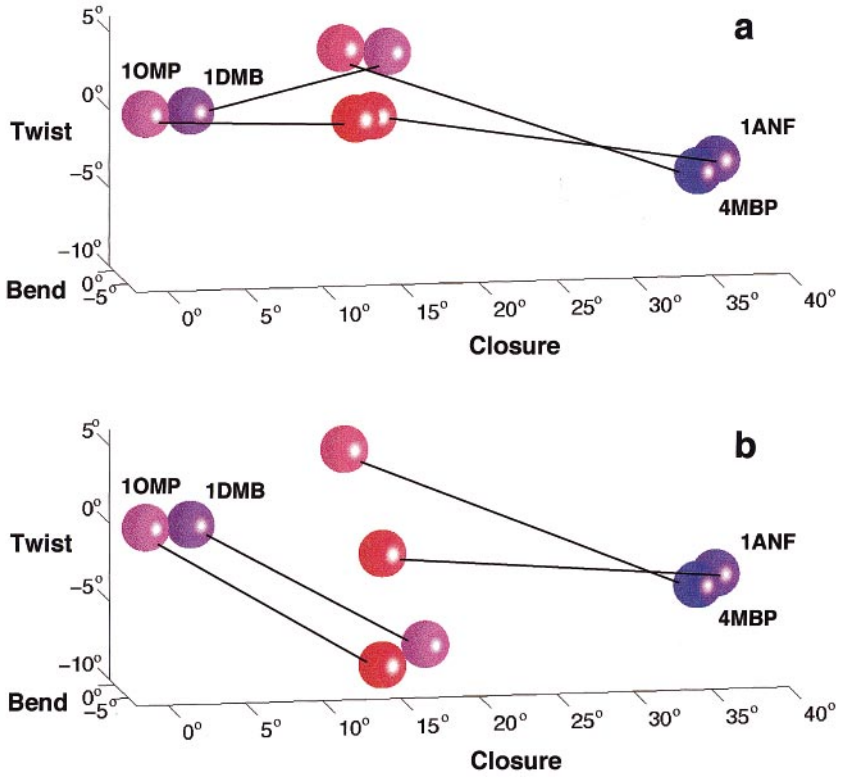

Figure 1. Schematic representation of the results from application of the conformational search algorithm to MBP. Spheres represent four published X-ray crystal structures and four solution structures which were derived (a) without considering interdomain dynamics or (b) assuming that the N-domain undergoes axial fluctuations about the hinge axis, as described in the text. All conformations are defined relative to the reference structure 1OMP (origin) *via* the sequence of three orthogonal rotations: closure, twist, and bending (in that particular order). This allows for a good visualization of the results owing to the near-commutativity of small rotations. For definitions of the closure, twist, and bending axes see Materials and Methods. The coloring scheme is based on χ^2 values (see Table 1) and thus represents the quality of the fit of experimental DC values to the indicated structure (red color corresponds to low χ^2). The experimental data are from α-helices and β-sheets within the N and C-domains; similar results are obtained when data for turn and loop regions are included.

mations were obtained (Figure 2(c) and (d)). The axis of hinge rotation that relates a solution structure to its parent crystal structure is indicated by an arrow for each crystalline form. Somewhat unexpectedly, the least successful solution structure is obtained from the β-cyclodextrin-bound crystal form of MBP (1DMB). As discussed below, this can be attributed to subtle, yet not inconsequential, local structural variations.

It should be noted that although the orientation of the hinge axis and the amplitude of opening and closure are determined directly from the experimental data, the position of the pivot (''effective hinge'') cannot be determined from dipolar couplings and must be obtained from other sources. The solution structures shown in Figures 2(c) and (d) were built using pivot coordinates obtained from analyses of open and closed X-ray crystal structures 1OMP and 1ANF as described in Materials and Methods. The rmsd between structures 2(c) and 2(d) is 1.8 Å for heavy backbone atoms in the repositioned N-domains.

Effect of local structural differences

The accuracy of the resulting solution structure was estimated in a series of test computations employing simulated DC data sets. For example, in one such simulation the DC values were calculated for a closed crystal structure, 1ANF. These values were subsequently used to reorient the domains of the open crystal structure, 1OMP, and thus reproduce the closed conformation. Applying our algorithm to pairs of open and closed crystal structures in this manner, the original crystal conformations were recovered with an average accuracy of $\pm 1^\circ$, $\pm 4^\circ$ and $\pm 2^\circ$ for closure, twist, and bending, respectively. This translates into a 1.7 Å average rmsd between the N-domains of original and reconstructed structures if the pivot coordinates are taken to be the same as above.

The discrepancy between the original and reconstructed conformations is due to the differences in local intradomain structure between the crystal forms of MBP. Such differences are subtle, as

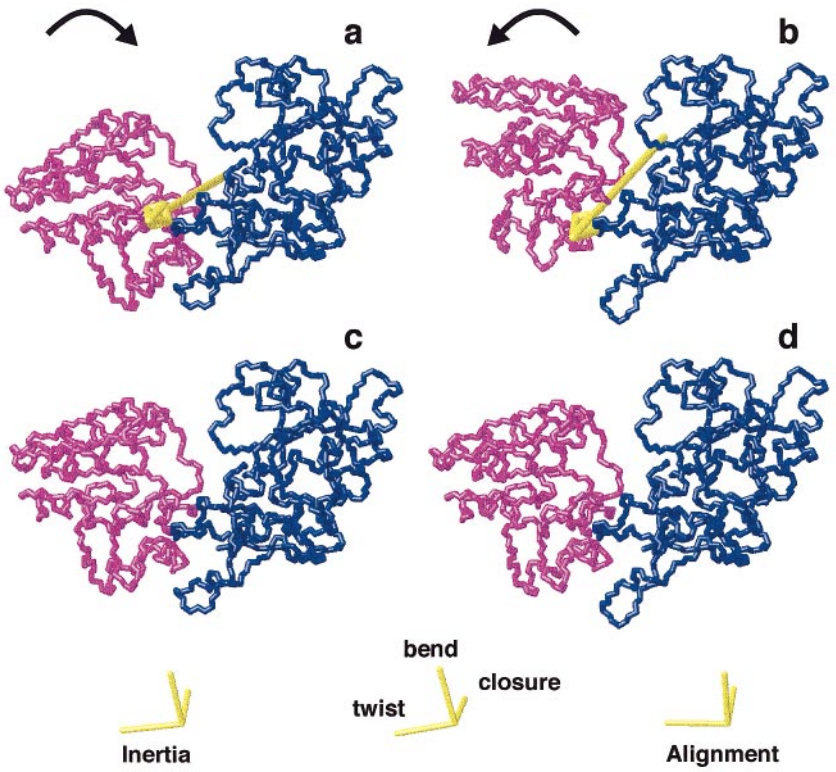

Figure 2. Backbone representation of MBP structures before and after application of the conformational search algorithm. Two crystal structures of maltodextrin-binding protein, (a) 1OMP and (b) 1ANF, and two representations of the solution structure of MBP with β-cyclodextrin, (c) and (d), generated from 1OMP and 1ANF, respectively, are illustrated. The N-domain (purple) is comprised of residues 6-109 and 264-309; the C-domain (blue) is comprised of residues 114-258 and 316-370. Also shown are the axes of hinge rotations that relate X-ray structures to the solution structures (yellow arrows), the axes of closure, twist, and bending, the principal axes of the tensor of inertia, and the principal axes of the alignment tensor for the solution structure (c).

characterized by an average rmsd of 0.4 Å (calculated for heavy backbone atoms from superimposed N-domains of open and closed structures) and the angle rmsd of 5° (calculated for N-H^N, N-C′, C^α-C′, C′-H^N, and C^α-H^N vectors from superimposed N-domains of open and closed structures), yet they introduce non-negligible errors in the outcome of the conformational search. Errors of similar magnitude are obtained when starting X-ray coordinates contain ''structural noise'' (e.g. random 5° tilt is applied to internuclear vectors).

The level of accuracy obtained in these test computations is quite similar to the precision achieved in the analysis of experimental data (Figure 1(a)). This suggests that the accuracy of our approach is limited by slight differences in the intradomain structure between various crystal forms of MBP and similar differences between the crystal structures and the average solution structure. By comparison, modest errors in experimental DC data appear to be less important. This has been verified in an additional series of computations where normally distributed random noise was added to the simulated DC data. Using the experimental errors reported by Yang *et al*. (1999) to specify the standard deviations of the simulated noise, we estimated the resulting uncertainty in closure, twist, and bending to be approximately 0.2°, 0.8°, and 0.2°, respectively. It has also been found that the adverse effect of small structural distortions can become severe if the number of utilized DC values drops below approximately 50 data points per domain (whereupon multiple minima tend to emerge in parameter space). Finally, the superior sensitivity to closure relative to twist observed in these studies is not surprising, since the long axis of the alignment tensor is nearly parallel with the twist axis (Figure 2), and therefore detection of twist relies on the small rhombic component, $R = 0.17$ (cf. equation (1)).

Potential effect of interdomain motion

It has recently been suggested that some periplasmic binding proteins show considerable flexibility in the open form such that many conformational species co-exist in solution in a state of dynamic equilibrium (Mowbray & Sandgren, 1998). In order to estimate the significance of these effects, a number of models describing interdomain dynamics have been considered.

In the first model, the protein is represented by two species: an open form ***a*** and a closed form ***b*** with fractional populations p_a and $p_b = 1 - p_a$, respectively. Assuming that there is rapid interconversion between the two forms, DCs can then be calculated as $D_{IM} = p_a D^a_{IM} + (1 - p_a) D^b_{IM}$. This model has been applied to β-cyclodextrin-loaded MBP, where the crystal structures 1OMP and 1ANF were used to represent the states ***a*** and ***b***, respectively (although there is no evidence that such two-state equilibrium occurs in MBP, this system is useful for model calculations). Upon fitting the experimental DC data using distinct sets of alignment parameters for species ***a*** and ***b***, we obtained $p_a A^a_a / (1 - p_a) A^b_a = 1.67$. This result indi-

cates that the average solution-state conformation is closer to the open state ***a*** than to the closed state ***b***, assuming that A_a^a and A_a^b are approximately equal. It is consistent with the results of Figure 1(a) where the above parameter can be estimated in a simple manner to be 1.65 (this value is obtained as a ratio of the closure angles between the average solution conformation and conformers 1ANF and 1OMP, respectively, $23^\circ/14^\circ = 1.65$). The results suggest that (i) measured DCs are adequately fitted using a single structure and no meaningful improvement is achieved by using a two-state model, and (ii) for proteins that are known to adopt two (or more) moderately different conformations in solution, the single structure obtained with our approach accurately represents the average, effective conformation. Note also that using this two-state model it is impossible to separate the fractional populations p_a, $p_b = 1 - p_a$ from the alignment parameters A_a^a, A_a^b.

In addition, we considered a model involving a multitude of conformational species. In this model, MBP undergoes interdomain motion (such as dynamic opening and closure). It is assumed that all conformers can be described using a single set of alignment parameters, and that the amplitude of motion relative to the alignment frame is the same for N and C-domains, which are approximately equal in size. While the first assumption may be an oversimplification (Emsley & Luckhurst, 1980), any attempt to express the alignment tensor as a function of variable protein conformation is not currently feasible, since relatively little is known about the mechanism of alignment. Under these assumptions, it is possible to demonstrate (see Materials and Methods) that the presence of interdomain dynamics leads to a modification of the alignment parameters, while the structural parameters determined in our approach (Table 1A and Figure 1(a)), remain unchanged.

We also have considered an alternative scenario where only the N-domain is mobile in the alignment frame. Although this model is not likely to be relevant for MBP in solution with Pf1 phage, it is included as a point of interest, since it represents a situation where interdomain motion may potentially affect the outcome of the conformational analysis. The amplitude of the axial fluctuations for the N-domain was set to $\pm 20^\circ$, which likely overestimates the amount of interdomain motion which could be present in MBP. The results of the conformational search are illustrated in Figure 1(b) where each of the four spheres in the center of the graph represents the mean conformation of the protein undergoing dynamic opening and closure (see Materials and Methods). The average conformation determined in this manner is characterized by $12(\pm 2)^\circ$ closure, $-3(\pm 6)^\circ$ twist, and $-2(\pm 3)^\circ$ bending relative to 1DMB (see Table 1B). Thus, interdomain motion manifests itself as ''dynamic noise'', which mainly affects the poorly known twist component but does not lead to any statistically significant change in the conformation determined in Figure 1(a). In summary, DC-based conformational analyses appear rather insensitive to intramolecular motion, and the quality of the mean solution-state conformation obtained is more likely to suffer from ''structural noise'' and limited number of measured DC constants than from dynamic noise.

Solution-state conformation of MBP

According to X-ray crystallographic studies, MBP bound to β-cyclodextrin exists in an open state (in this form the protein is unable to stimulate sugar uptake (Sharff *et al.*, 1993)). In the crystal structure (1DMB), one side of β-cyclodextrin makes numerous binding contacts to MBP *via* the C-domain, while the other side of β-cyclodextrin is heavily hydrated and has few interactions with the N-domain. The solution structure produced here shows much closer association between the ligand and the N-domain, with a concomitant decrease in the solvent-accessible surface area in the binding cleft. The reconstructed complex of MBP with β-cyclodextrin does not show any steric violations for protein backbone atoms, although a small number of conflicts do arise between N-domain side-chains and β-cyclodextrin. These violations can be eliminated by reorienting a few side-chains (e.g. rotations about χ_2 in Lys42 and χ_1 in Asp14 are the only changes required to accommodate β-cyclodextrin in the solution structure shown in Figure 2(c) and (d)).

Although the solution-state conformation obtained here is certainly reasonable in terms of accommodating the ligand, it is possible that the closure observed in β-cyclodextrin-bound MBP in solution could, in fact, be induced by transient site-specific binding of the protein to Pf1 phage. However, this is unlikely, since the alignment of MBP in phage appears to be the result of non-specific collision-type processes involving protein and phage (Tjandra & Bax, 1997; de Alba *et al.*, 1999). Indeed, the principal axes of the alignment tensor for MBP are nearly parallel with the principal axes of the ellipsoid of inertia (Figure 2) with the two long axes making an angle of only 8°. This suggests that site-specific binding to phage does not occur and that the conformation of β-cyclodextrin-bound MBP observed in anisotropic phage solvent also represents the conformation existing in isotropic physiological solutions. The high quality of spectra recorded for MBP in Pf1 phage solvent (Yang *et al.*, 1999) and the small magnitude of dipolar couplings observed at low phage concentrations (under 5 mg/ml) are consistent with a transient, non-specific character of protein-phage interaction (Ojennus *et al.*, 1999). More information about protein-phage interactions can potentially be obtained from spin relaxation measurements (Bax & Tjandra, 1997; North *et al.*, 1994).

The difference between X-ray and solution structures of the MBP-β-cyclodextrin complex can be attributed to crystal packing interactions, which

are thought to be extensive in this form of MBP (Spurlino *et al.*, 1991; Sharff *et al.*, 1993). Discrepancies between X-ray and solution structures have also been described for the galactose- and ribose-binding proteins (Shilton *et al.*, 1996; Björkman & Mowbray, 1998), which are two other members of the periplasmic binding protein family. The data obtained in spin-labeling studies (Hall *et al.*, 1997) indicate that MBP shows noticeable closure upon binding β-cyclodextrin in solution, which is consistent with our findings. Our analysis of anisotropic rotational tumbling based on ^{15}N relaxation parameters (Brüschweiler *et al.*, 1995; Lee *et al.*, 1997; Tjandra *et al.*, 1996b) also confirms that the solution-state conformation of β-cyclodextrin-loaded MBP is more closed than the crystal form, albeit within a wide range of uncertainty (5-20° closure). The present results demonstrate that NMR dipolar coupling measurements can be combined with X-ray crystallographic data to accurately determine the relative orientation of domains in solution, necessary to understand the many types of protein function that involve domain rearrangement.

Materials and Methods

Preparation of the sample of ^{15}N, ^{13}C, ^{2}H-labeled MBP with β-cyclodextrin in Pf1 phage liquid-crystalline solvent (Hansen *et al.*, 1998) (concentration of Pf1 phage 19 mg/ml) and the TROSY-based HNCO experiments used for measurement of the dipolar couplings were as described previously (Yang *et al.*, 1999). The data were obtained for one-bond ^{15}N-H^N (280), ^{15}N-$^{13}C'$ (262), $^{13}C^{\alpha}$-$^{13}C'$ (276), two-bond $^{13}C'$-H^N (262), and three-bond $^{13}C^{\alpha}$-H^N (276) DC constants. Tables containing the measured DC values will be available on our website at http://abragam.med.utoronto.ca.

Prior to the analysis, the X-ray structures of MBP were placed into the same coordinate frame by fitting their C-domains using the structure analysis program MOLMOL (Koradi *et al.*, 1996). In this study, all structures have been transferred into the coordinate frame of 1OMP, although any other coordinate system could have been used as well. Protons were added to the atomic coordinate set with MOLMOL. A separate fitting program was written to determine the parameters of hinge rotation relating two crystal structures. Using this program, we established the coordinates of the pivot for the hinge rotation that relates 1OMP and 1ANF. It is worth noting that, in general, only two pivot coordinates out of three must be determined (e.g. an intersection of the hinge axis with the *xy* plane). The hinge axis obtained in our analysis of the 1OMP/1ANF pair goes through the interdomain region of the protein in close proximity to two linker β-strands (within 2 Å of the center of mass of peptide planes of residues 111 and 261 (Sharff *et al.*, 1992)). In the coordinate frame of 1OMP, the orientation of the hinge axis is given by the polar angles (102°, 123°), and the pivot can be localized, for example, at the point with *x*, *y*, *z* coordinates [1.53, 1.04, −2.79].

The closure, twist, and bending axes have been introduced in the following fashion. The twist axis is defined as a line connecting the centers of mass of the N and C-domains in the reference structure 1OMP (deGroot *et al.*, 1998). The closure axis is derived from the axis of rotation that transforms 1ANF into 1OMP (see above), subject to orthogonalization with respect to the twist axis. The bending axis is formed as a cross-product of the twist and closure axes. The decomposition of the hinge rotations into closure, twist, and bending is useful for small-amplitude rotations; it offers less insight for large-amplitude rotations because closure, twist, and bending do not commute.

The relative orientation of the domains of MBP in solution was determined using a conformational search algorithm that functions as follows. First, all X-ray structures are placed in the same coordinate frame by superimposing their C-domains as described above. The internuclear vectors $\vec{v}_{IM}$ for which experimental DC values are available are subsequently extracted from the coordinate files. A new molecular conformation is then generated by applying a hinge rotation to all vectors from the N-domain, $\vec{v}^{N}_{IM}$, while leaving the vectors from the C-domain, $\vec{v}^{C}_{IM}$, unchanged. A hinge rotation with amplitude ω about the axis $\vec{n}$ is described by the following equation (Varshalovich *et al.*, 1988):

$$\vec{v}'^{N}_{IM} = \vec{v}^{N}_{IM}\cos\omega + \vec{n}(\vec{n}\cdot\vec{v}^{N}_{IM})(1-\cos\omega) + [\vec{n}\times\vec{v}^{N}_{IM}]\sin\omega \quad (2)$$

where $\vec{v}'^{N}_{IM}$ denotes the rotated vector and the orientation of $\vec{n}$ is specified in the fixed coordinate frame described above, $\vec{n} = (\sin\Theta\cos\Phi, \sin\Theta\sin\Phi, \cos\Theta)$. The set of internuclear vectors $\{\vec{v}'^{N}_{IM}, \vec{v}^{C}_{IM}\}$ is then transformed into a new coordinate frame, which represents a potential alignment frame, using a standard transformation matrix parametrized by Euler angles α, β, γ (see equation (54), p.30 of Varshalovich *et al.*, 1988). The resulting vector orientations are expressed in terms of polar angles θ, ϕ and used to calculate dipolar couplings according to equation (1). The deviation between the calculated and experimental DC values is subsequently computed as a sum over all measured spin pairs, $\chi^2 = \sum_i (D^{i\ calc}_{IM} - D^{i\ exptl}_{IM})^2$, where the individual terms also can be weighted according to the error in measured DC values.

These computations are iterated within a simplex minimization algorithm for χ^2, thereby fitting three structural parameters, Θ, Φ, ω, together with five alignment parameters, A_a, R, α, β, γ (see equation (1)). The input data for MBP include 1356 measured DC values and the corresponding number of polar angles that define the orientation of internuclear dipole vectors in the X-ray coordinate frame. The minimization is repeated several times starting from randomized initial conditions in order to ensure that the global minimum is found (this can be also verified by viewing cross-sections of the χ^2 hypersurface). The program, named Conformist1.0, was written using MATLAB software (MathWorks Inc.) and is supplied with a graphical user interface.

An alternative approach, also implemented in Conformist1.0, independently fits two sets of alignment parameters for N and C-domains: A^N_a, R^N, α^N, β^N, γ^N and A^C_a, R^C, α^C, β^C, γ^C (Fischer *et al.*, 1999). Differences between the alignment tensor orientations given by $\{\alpha^N, \beta^N, \gamma^N\}$ and $\{\alpha^C, \beta^C, \gamma^C\}$ can be used to determine the conformational changes between the X-ray and solution forms (also formulated in terms of hinge rotations). Throughout this study, the results from the two approaches were found to be virtually identical. The parameters of alignment tensors for the two domains were very close (e.g. $A^N_a = 1.524\times10^{-3}$, $R_N = 0.161$, and $A^C_a = 1.526\times10^{-3}$, $R^C = 0.182$ for the solution structure derived from 1OMP) thus confirming that local

dynamics in the two domains is similar and molecular alignment is appropriately described by single values of A_a and R. This conclusion is supported by heteronuclear ^{1}H-^{15}N steady-state NOE data which show the same average values (0.77) for the N and C-domains. The fact that alignment parameters are similar for the two domains of MBP is not enough to rule out the possibility of interdomain dynamics because the domains, which are approximately equal in size, may display the same amount of motion (see the section discussing interdomain motion). However, this result does rule out the worst-case scenario where one of the domains binds to phage, while the other domain remains highly mobile (Fischer *et al*., 1999).

The effects of interdomain dynamics were investigated by incorporating dynamic effects into equation (1). In these analyses, the conformation generated according to equation (2) is subject to interdomain motion in the form of axial fluctuations about an arbitrary axis $\vec{d}$ which are fast on the time-scale of D_{IM}^{-1}. We assumed that this dynamic system can be described using a single set of alignment parameters, valid only if interdomain motion does not interfere with alignment processes. Since the alignment and inertia frames are near coincident (reflecting the absence of site-specific binding to the phage) and the two domains of MBP are approximately equal in size, it is reasonable to suggest that the motion for the N and C-domains relative to the alignment frame is similar. Consequently, the motion of the two domains can be described by a single equilibrium probability distribution $P(\delta)$, where $\delta(t)$ is the amplitude of axial fluctuations with zero average value, $\langle\delta\rangle = 0$. For this model, the expected DC values can be readily calculated if equation (1) is reformulated in terms of spherical harmonics $Y_{2l}(\theta, \phi)$ subject to averaging with distribution $P(\delta)$ in accordance with the following equations:

$$D_{IM} = D_0^{IM} A_a S \sqrt{\frac{16\pi}{5}} \left\{ \langle Y_{20}(\theta, \phi)\rangle + \sqrt{\frac{3}{8}} R(\langle Y_{22}(\theta, \phi)\rangle + \langle Y_{2-2}(\theta, \phi)\rangle) \right\} \quad (3)$$

$$\langle Y_{2l}(\theta, \phi)\rangle = \sum_{m,m',n,n'=-2}^{2} \mathcal{D}^{(2)}_{ml}(\alpha, \beta, \gamma)\mathcal{D}^{(2)}_{m'm}(0, -\Psi, -\Omega) F_{m'}(P)\mathcal{D}^{(2)}_{m'm'}(\Omega, \Psi, 0)\mathcal{D}^{(2)}_{nn'}(-\gamma, -\beta, -\alpha)Y_{2n}(\theta, \phi) \quad (4)$$

where $\mathcal{D}^{(2)}$ denotes the ij element of a second-rank Wigner matrix defined in terms of a passive rotation (Varshalovich *et al*., 1988), $F_k(P)$ is given by $\int_{-\pi}^{\pi} P(\delta)e^{ik\delta}d\delta / \int_{-\pi}^{\pi} P(\delta)d\delta$, and polar angles Ψ, Ω specify the orientation of the hinge axis $\vec{d}$ in the X-ray coordinate frame. Substitution of equation (4) into equation (3) shows that D_{IM} is given by a linear combination of the spherical harmonics $Y_{2n}(\theta, \phi)$ with the coefficients independent of θ and ϕ. Therefore, it is always possible to find the coordinate frame where the above result is reduced to the form of equation (1). This frame can be viewed as an alignment frame which has been modified by intramolecular motion, with A_a and R changed accordingly. Consequently, equations (3) and (4) are equivalent to equation (1) in the context of the conformational search algorithm, leading to identical values of Θ, ϕ, and ω. However, if equations (3) and (4) are applied selectively (e.g. only to the N-domain) then the equivalence breaks down and the results for Θ, ϕ, ω can be affected by interdomain motion. This situation is illustrated in Figure 1(b) where solution-state conformations were derived employing equations (3) and (4) to calculate the dipolar couplings in the N-domain. The calculations were carried out for $\vec{d} = \vec{n}$ assuming that $P(\delta) = 1/(2\Delta)$ in the interval $-\Delta < \delta < \Delta$ and zero elsewhere, $F_k(P) = \sin(k\Delta)/(k\Delta)$, and using the value $\Delta = 20^\circ$.

Acknowledgments

This research has been supported by the Medical Research Council of Canada. L.E.K. is a foreign investigator of the Howard Hughes Medical Research Institute.

References

Bastiaan, E. W., MacLean, C., van Zijl, P. C. M. & Bothner-By, A. A. (1987). High resolution NMR of liquids and gases: effects of magnetic-field-induced molecular alignment. *Annu. Rep. NMR Spectrosc.* **9**, 35-77.

Bax, A. (1994). Multidimensional nuclear magnetic resonance methods for protein studies. *Curr. Opin. Struct. Biol.* **4**, 738-744.

Bax, A. & Tjandra, N. (1997). High-resolution heteronuclear NMR of human ubiquitin in an aqueous liquid crystalline medium. *J. Biomol. NMR,* **10**, 289-292.

Björkman, A. J. & Mowbray, S. L. (1998). Multiple open forms of ribose-binding protein trace the path of its conformational change. *J. Mol. Biol.* **279**, 651-664.

Brüschweiler, R., Liao, X. B. & Wright, P. E. (1995). Long-range motional restrictions in a multidomain zinc-finger protein. *Science,* **268**, 886-889.

Clore, G. M., Gronenborn, A. M. & Bax, A. (1998). A robust method for determining the magnitude of the fully asymmetric alignment tensor of oriented macromolecules in the absence of structural information. *J. Magn. Reson.* **133**, 216-221.

de Alba, E., Baber, J. L. & Tjandra, N. (1999). The use of residual dipolar coupling in concert with backbone relaxation rates to identify conformational exchange by NMR. *J. Am. Chem. Soc.* **121**, 4282-4283.

deGroot, B. L., Hayward, S., van Aalten, D. M. F., Amadei, A. & Berendsen, H. J. C. (1998). Domain motions in bacteriophage T4 lysozyme: a comparison between molecular dynamics and crystallographic data. *Proteins: Struct. Funct. Genet.* **31**, 116-127.

Emsley, J. W. & Luckhurst, G. R. (1980). The effect of internal motion on the orientational order parameters for liquid crystalline systems. *Mol. Phys.* **41**, 19-29.

Fischer, M. W. F., Losonczi, J. A., Weaver, J. L. & Prestegard, J. H. (1999). Domain orientation and dynamics in multidomain proteins from residual dipolar couplings. *Biochemistry,* **38**, 9013-9022.

Gardner, K. H. & Kay, L. E. (1998). The use of ^{2}H, ^{13}C, ^{15}N multidimensional NMR to study the structure and dynamics of proteins. *Annu. Rev. Biophys. Biomol. Struct.* **27**, 357-406.

Gardner, K. H., Zhang, X., Gehring, K. & Kay, L. E. (1998). Solution NMR studies of a 42 kDa *Escherichia coli* maltose binding protein/β-cyclodextrin complex: chemical shift assignments and analysis. *J. Am. Chem. Soc.* **120**, 11738-11748.

Gerstein, M., Lesk, A. M. & Chothia, C. (1994). Structural mechanisms for domain movements in proteins. *Biochemistry,* **33**, 6739-6749.

Hall, J. A., Thorgeirsson, T. E., Liu, J., Shin, Y.-K. & Nikaido, H. (1997). Two models of ligand binding in maltose-binding protein of *Escherichia coli*. *J. Biol. Chem.* **272**, 17610-17614.

Hansen, M. R., Mueller, L. & Pardi, A. (1998). Tunable alignment of macromolecules by filamentous phage yields dipolar coupling interactions. *Nature Struct. Biol.* **5**, 1065- 1074.

Koradi, R., Billeter, M. & Wüthrich, K. (1996). MOLMOL: a program for display and analysis of macromolecular structures. *J. Mol. Graph.* **14**, 51-55.

Lee, L. K., Rance, M., Chazin, W. J. & Palmer, A. G. (1997). Rotational diffusion anisotropy of proteins from simultaneous analysis of ^{15}N and $^{13}C^{\alpha}$ nuclear spin relaxation. *J. Biomol. NMR,* **9**, 287-298.

Losonczi, J. A., Andrec, M., Fischer, M. W. F. & Prestegard, J. H. (1999). Order matrix analysis of residual dipolar couplings using singular value decomposition. *J. Magn. Reson.* **138**, 334-342.

Markus, M. A., Gerstner, R. B., Draper, D. E. & Torchia, D. A. (1999). Refining the overall structure and subdomain orientation of ribosomal protein S4 Δ41 with dipolar couplings measured by NMR in uniaxial liquid crystalline phases. *J. Mol. Biol.* **292**, 375-387.

Mowbray, S. L. & Sandgren, M. O. J. (1998). Chemotaxis receptors: a progress report on structure and function. *J. Struct. Biol.* **124**, 257-275.

North, C. L., Franklin, J. C., Bryant, R. G. & Cafiso, D. S. (1994). Molecular flexibility demonstrated by paramagnetic enhancements of nuclear relaxation. Application to alamethicin: a voltage-gated peptide channel. *Biophys. J.* **67**, 1861-1866.

Ojennus, D. D., Mitton-Fry, R. M. & Wuttke, D. S. (1999). Induced alignment and measurement of dipolar couplings of an SH2 domain through direct binding with filamentous phage. *J. Biomol. NMR,* **14**, 175-179.

Pawson, T. (1995). Protein modules and signalling networks. *Nature,* **273**, 573-580.

Quiocho, F. A., Spurlino, J. C. & Rodseth, L. E. (1997). Extensive features of tight oligosaccharide binding revealed in high-resolution structures of the maltodextrin transport/chemosensory receptor. *Structure,* **5**, 997-1015.

Sharff, A. J., Rodseth, L. E., Spurlino, J. C. & Quiocho, F. A. (1992). Crystallographic evidence of a large ligand-induced hinge-twist motion between the two domains of the maltodextrin binding protein involved in active transport and chemotaxis. *Biochemistry,* **31**, 10657-10663.

Sharff, A. J., Rodseth, L. E. & Quiocho, F. A. (1993). Refined 1.8-Å structure reveals the mode of binding of β-cyclodextrin to the maltodextrin binding protein. *Biochemistry,* **32**, 10553-10559.

Shilton, B. H., Flocco, M. M., Nilsson, M. & Mowbray, S. L. (1996). Conformational changes of three periplasmic receptors for bacterial chemotaxis and transport: the maltose-, glucose/galactose- and ribose-binding proteins. *J. Mol. Biol.* **264**, 350-363.

Spurlino, J. C., Lu, G.-Y. & Quiocho, F. A. (1991). The 2.3-Å resolution structure of the maltose or maltodextrin-binding protein, a primary receptor of bacterial active transport and chemotaxis. *J. Mol. Biol.* **264**, 350-363.

Tjandra, N. & Bax, A. (1997). Direct measurement of distances and angles in biomolecules by NMR in a dilute liquid crystalline medium. *Science,* **278**, 1111-1114.

Tjandra, N., Grzesiek, S. & Bax, A. (1996a). Magnetic field dependence of nitrogen-proton J splittings in ^{15}N-enriched human ubiquitin resulting from relaxation interference and residual dipolar coupling. *J. Am. Chem. Soc.* **118**, 6264-6272.

Tjandra, N., Wingfield, P., Stahl, S. & Bax, A. (1996b). Anisotropic rotational diffusion of perdeuterated HIV protease from ^{15}N NMR relaxation measurements at two magnetic fields. *J. Biomol. NMR,* **8**, 273-284.

Tolman, J. R., Flanagan, J. M., Kennedy, M. A. & Prestegard, J. H. (1995). Nuclear magnetic dipole interactions in field-oriented proteins: information for structure determination in solution. *Proc. Natl Acad. Sci. USA,* **92**, 9279-9283.

Van Aalten, D. M. F., Conn, D. A., De Groot, B. L., Findlay, J. B. C., Berendsen, H. J. C. & Amadei, A. (1997). Protein dynamics derived from clusters of crystal structures. *Biophys. J.* **73**, 2891-2896.

Varshalovich, D. A., Moskalev, A. N. & Khersonskii, V. K. (1988). *Quantum Theory of Angular Momentum: Irreducible Tensors, Spherical Harmonics, Vector Coupling Coefficients, 3nj Symbols*, World Scientific Publishing, Singapore.

Wang, Y. X., Marquardt, J. L., Wingfield, P., Stahl, S. J., Lee-Huang, S., Torchia, D. & Bax, A. (1998). Simultaneous measurement of ^{1}H-^{15}N, ^{1}H-$^{13}C'$, and ^{15}N-$^{13}C'$ dipolar couplings in a perdeuterated 30 kDa protein dissolved in a dilute liquid crystalline phase. *J. Am. Chem. Soc.* **120**, 7385-7386.

Yang, D. & Kay, L. E. (1999). TROSY triple-resonance four-dimensional NMR spectroscopy of a 46 ns tumbling protein. *J. Am. Chem. Soc.* **121**, 2571-2575.

Yang, D., Venters, R. A., Mueller, G. A., Choy, W. Y. & Kay, L. E. (1999). TROSY-based HNCO pulse sequence for the measurement of ^{1}HN-^{15}N, ^{15}N-^{13}CO, ^{1}HN-^{13}CO, ^{13}CO-$^{13}C^{\alpha}$, and ^{1}HN-$^{13}C^{\alpha}$ dipolar couplings in ^{15}N, ^{13}C, ^{2}H labeled proteins. *J. Biomol. NMR,* **14**, 333-343.

Zwahlen, C., Gardner, K. H., Sarma, S. P., Horita, D. A., Byrd, R. A. & Kay, L. E. (1998). An NMR experiment for measuring methyl-methyl NOEs in ^{13}C-labeled proteins with high resolution. *J. Am. Chem. Soc.* **120**, 7617-7625.

Edited by P. E. Wright

(Received 30 September 1999; received in revised form 29 November 1999; accepted 29 November 1999)